ICAS 2016
30th Congress of the International Council of the Aeronautical Sciences
DCC, Daejeon, Korea ; September 25-30, 2016

CAPTURE REGION ANALYSIS FOR MISSILE GUIDANCE WITH FIELD-OF-VIEW CONSTRAINT AGAINST MOVING TARGET

Seokwon Lee *, Youdan Kim*, and Tae-Yoon Um**
***Department of Mechanical and Aerospace Engineering, Seoul National University, Seoul, 151-742, Republic of Korea**
****Agency for Defense Development, Daejeon 305-600, Republic of Korea**

Keywords: FOV (Field-of View), Missile Guidance, Strapdown seeker

Abstract

A capture region for missile guidance laws under field-of-view constraint is analyzed. To make a missile intercept a non-maneuvering target, physical constraints including seeker`s field-of-view and acceleration limit should be considered, because these constraints may restrict maneuver of the interceptor. The characteristics of look-angle constraint guidance laws is studied, and feasible trajectory envelope and achievable impact angle set are derived using deviated pursuit trajectory. To validate the analysis of the capture region, numerical simulation is carried out.

1 Introduction

Strapdown-seeker system has several advantages over gimbal-seeker system because of its simple mechanic structure, low-cost, and light weight. For these reasons, the strapdown-seeker system has been widely utilized in guided weapons including guided projectiles, kill vehicles, and missiles.

For missiles equipped with strapdown-seeker, maintaining lock-on is crucial because a target information is directly obtained from the seeker. The seeker is attached to the missile body and the FOV (Field-of-View) of the seeker is limited, and therefore the missile maneuver and its reachable trajectory may be restricted. Usually, missile with a strapdown-seeker requires a guidance law that can maintain lock-on condition and also satisfy terminal homing objectives. To design guidance law for a missile considering FOV limit, two-stage guidance law [1-3], optimal guidance law [4], biased proportional navigation guidance [5], and hybrid guidance scheme [6] have been proposed. Most of the previous studies, however, focused on stationary target interception [1-5], or slow-moving target interception with wide FOV limit. [6,7]

The objective of this study is to find a necessary condition for capture region of the look-angle constraint guidance laws. First, the property of the look-angle constraint guidance law is analyzed where the maximum maneuver of the missile is restricted to maintain the lock-on condition. Then, a feasible trajectory envelope is derived from the pursuit trajectory. Based on the obtained envelope boundary, qualitative behavior of the maximum trajectory is analyzed for tail-chase and head-on engagement cases. The impact angle set can be determined, and necessary condition for the capturable region is examined. To demonstrate the analysis result using the capture region, numerical simulations are performed.

This paper is organized as follows. Section 2 presents the problem formulation and characteristics of look-angle constraint guidance. Section 3 provides the capture region analysis. Numerical simulation results are shown in Sec. 4, Finally, conclusion is given in Sec. 5.

2 Problem formulation

2.1 Engagement Kinematics

Consider a planar engagement geometry as shown in Fig. 1, where the subscript T and subscript M denote the target and the missile, respectively. In this study, the missile and the target are assumed as point mass model with constant speed V_T and V_m . The following assumptions are used for the analysis in this study.

Assumption 1: A missile and a target maneuver in planar motion.
Assumption 2: The target is non-maneuvering, and the speed is lower than that of the missile.
Assumption 3: The angle of attack (AOA) of the missile is small enough to be neglected.

From the Assumption 3, the pitch angle of the missile denoted by θ_m coincides with the flight path angle γ as

$$\theta_m = \gamma_m \tag{1}$$

Using Eq. (1), the look angle σ can be defined using the relation between LOS angle λ and the flight path angle γ_m as

$$\lambda = \sigma + \gamma_m \tag{2}$$

The nonlinear kinematics in the planar engagement can be represented as follows

$$\dot{r} = V_T \cos(\gamma_T - \lambda) - V_m \cos\sigma \tag{3}$$

$$\dot{\lambda} = \frac{V_T}{r}\sin(\gamma_T - \lambda) + \frac{V_m}{r}\sin\sigma \tag{4}$$

$$\dot{\sigma} = \frac{V_T}{r}\sin(\gamma_T - \lambda) + \frac{V_m}{r}\sin\sigma - \frac{a_m}{V_m} \tag{5}$$

where r denotes the distance between the missile and the target, γ_T indicates the flight path angle of the target, and a_m is the normal acceleration of the missile.

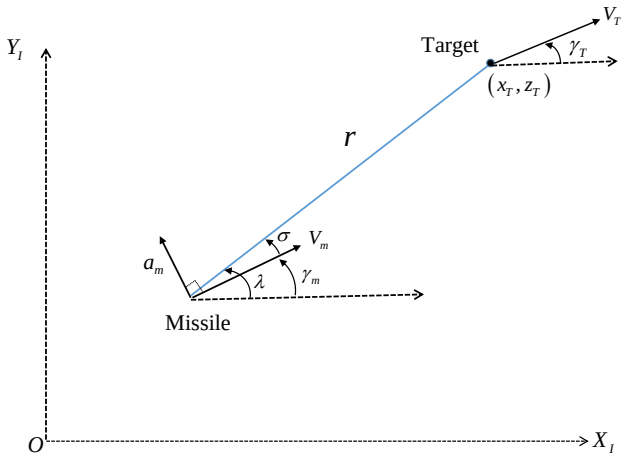

Figure 1 Planar Engagement geometry

2.2 Characteristics of Look-angle constraint guidance law

The look-angle constraint guidance laws considering FOV limit of the seeker have a common property that the maximum maneuver should be restricted to maintain its maximum look-angle. The guidance command of the missile can be represented as

$$a_{m_c} = \begin{cases} a_{c_{\text{homing}}} & \sigma_{\min} < \sigma < \sigma_{\max} \\ V_m\dot{\lambda} & \sigma = \sigma_{\max},\ \sigma = \sigma_{\min} \end{cases} \tag{6}$$

where $a_{c_{\text{homing}}}$ is a homing guidance command generated by the guidance schemes, and $(\sigma_{\max}, \sigma_{\min})$ are maximum/minimum look angles due to the FOV limit. If the look angle is remained within the FOV limit during the maneuver, the guidance command can make the missile intercept the target without interference of the FOV limit. In Refs. [1-5], pure-proportional navigation (PPN) was used as a homing guidance law. On the other hand, if the look angle reaches the maximum/minimum boundary, $\sigma = \sigma_{\max}$ or $\sigma = \sigma_{\min}$, and

$$\dot{\sigma} = 0 \tag{7}$$

The meaning of Eq. (7) is that the missile maneuver is constrained to maintain its look angle. Using Eqs. (3) and (4), the differential equation of LOS angle can be expressed with respect to r as

$$\frac{dr}{r}=\frac{V_T\cos(\gamma_T-\lambda)-V_m\cos\sigma_{\max}}{V_T\sin(\gamma_T-\lambda)+V_m\sin\sigma_{\max}}d\lambda \quad (8)$$

Since $\gamma_T=\gamma_T(0)$ for a non-maneuvering target and $\sigma=\sigma_{\max}$, Eq. (8) is equivalent to the ordinary differential equation of the deviated pursuit guidance trajectory. Integrating by part gives the analytic solution of the trajectory as

$$r=r_0\frac{V_T\sin(\gamma_T-\lambda_0)+V_m\sin\sigma_{\max}}{V_T\sin(\gamma_T-\lambda)+V_m\sin\sigma_{\max}}\times \exp\int_{\lambda_0}^{\lambda}\frac{-V_m\cos\sigma_{\max}}{V_T\sin(\gamma_T-\lambda)+V_m\sin\sigma_{\max}}d\lambda \quad (9)$$

The closed-form solution of the $\int_{\lambda_0}^{\lambda}\frac{-V_m\cos\sigma_{\max}}{V_T\sin(\gamma_T-\lambda)+V_m\sin\sigma_{\max}}d\lambda$ in Eq. (9) are different according to the speed ratio ($\eta=V_T/V_m$) as well as FOV limit $\sigma_{\max}$. By defining a parameter $a=\eta/\sin\sigma_{\max}$, the analytic solution can be obtained as

for $a<1$

$$\int_{\lambda_0}^{\lambda}\frac{-V_m\cos\sigma_{\max}}{V_T\sin(\gamma_T-\lambda)+V_m\sin\sigma_{\max}}d\lambda \quad (10)$$
$$=\frac{2\cot\sigma_{\max}}{\sqrt{1-a^2}}\tan^{-1}\left(\frac{\tan\left(\frac{\gamma_T-\lambda}{2}\right)+a}{\sqrt{1-a^2}}\right)\Bigg|_{\lambda_0}^{\lambda}$$

for $a>1$

$$\int_{\lambda_0}^{\lambda}\frac{-V_m\cos\sigma_{\max}}{V_T\sin(\gamma_T-\lambda)+V_m\sin\sigma_{\max}}d\lambda \quad (11)$$
$$=-\frac{2\cot\sigma_{\max}}{\sqrt{a^2-1}}\tanh^{-1}\left(\frac{\tan\left(\frac{\gamma_T-\lambda}{2}\right)+a}{\sqrt{a^2-1}}\right)\Bigg|_{\lambda_0}^{\lambda}$$

From Eqs. (9)-(11), the qualitative behavior of the solution varies according to the parameter a. Usually, if the target speed is much slower than missile speed and FOV limit is large, then $a<1$. If FOV is small, on the other hand, the parameter a becomes greater than unity.

2.3 Maximum acceleration constraint

To reflect the physical constraint of the missile, the maximum acceleration limit is considered. As the missile approaches the target while keeping the look angle within the allowable limit, the turning rate of the missile reaches its maximum. When the look angle keeps a constant σ_0, the relation between the maximum acceleration and LOS rate can be obtained as

$$\dot\gamma_{\max}=\frac{V_T}{r}\sin(\gamma_T-\lambda)+\frac{V_m}{r}\sin\sigma_0=\frac{a_{\max}}{V_m}$$
$$\dot\gamma_{\min}=\frac{V_T}{r}\sin(\gamma_T-\lambda)+\frac{V_m}{r}\sin\sigma_0=-\frac{a_{\max}}{V_m} \quad (12)$$

where $(a_{\max},a_{\min})$ are the maximum and minimum accelerations. Because $r>0$, Eq. (12) can be expressed as

$$r=\left|V_T\sin(\gamma_T-\lambda)+V_m\sin\sigma_0\right|\frac{V_m}{a_{\max}} \quad (13)$$

When the missile reaches its maximum acceleration, the missile cannot follow the target due to the maneuverability limit. It causes miss-distance and fails to lock-on the target. The maximum acceleration boundary of Eq. (13) should be used in the capture region analysis. Figures 2 and 3 show the phase portrait of the pursuit trajectory represented in LOS coordinates.

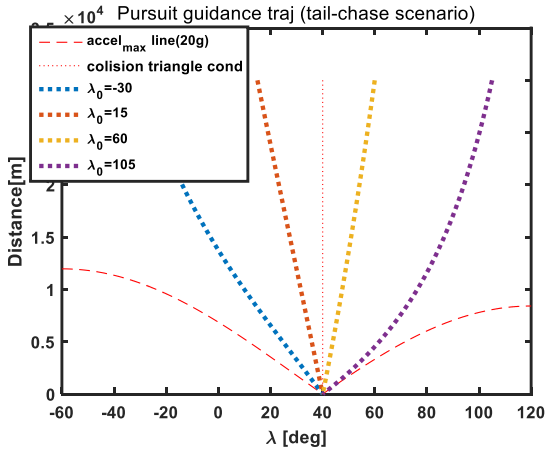

Figure 2 Phase portrait of pursuit trajectory (Tail-chase engagement case)

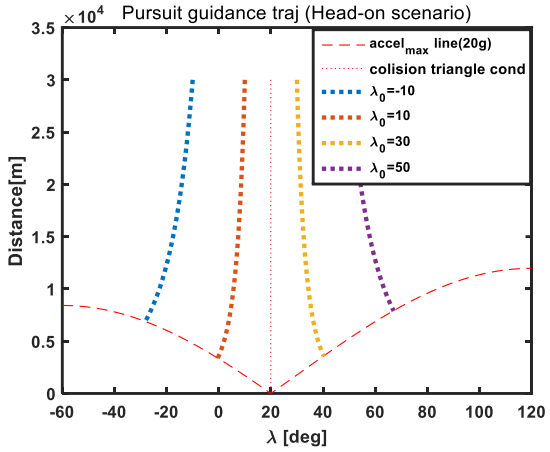

Figure 3 Phase portrait of pursuit trajectory (Head-on engagement case)

For a tail-chase engagement case, an attractive equilibrium point can be obtained by collision triangle condition as shown in Fig. 2. It ensures that any trajectory converges to the equilibrium point for any initial position. For a head-on engagement case, on the other hand, the LOS diverges from the unstable equilibrium point as the missile gets close to the target. The trajectory reaches the maximum acceleration boundary. After reaching the acceleration limit, the missile cannot intercept the target due to the limited maneuverability. Based on the result, capture region analysis can be performed, which will be described in the next section.

3 Capture Region Analysis

3.1 Achievable Impact angle

In this section, the achievable impact angle sets under FOV constraint is provided. At the end of the homing phase, the missile and the target should satisfy the condition of the collision course. Using Eqs. (2) and (4), the corresponding collision triangle condition can be obtained as follows

$$\begin{aligned} &V_T \sin\left(\gamma_T-\gamma_m-\sigma\right)+V_m \sin\sigma \\ &=V_T \sin\left(\gamma_T-\gamma_m\right)\cos\sigma \\ &+\left(V_m-V_T\cos\left(\gamma_T-\gamma_m\right)\right)\sin\sigma=0 \end{aligned} \tag{14}$$

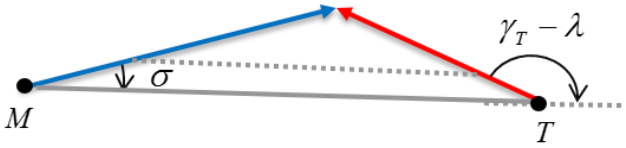

Figure 4 Collision Triangle

Figure 4 shows the configuration of the collision triangle condition. During the collision course, the missile and the target form a collision triangle to keep a constant LOS. To lock-on the target during this interval, the terminal look angle and corresponding terminal impact angle should be chosen according to the FOV limit. Rearranging Eq. (14) yields

$$\tan\sigma_f=\frac{V_T\sin\left(\gamma_T-\gamma_f\right)}{V_T\cos\left(\gamma_T-\gamma_f\right)-V_m}=\frac{\eta\sin\left(\gamma_T-\gamma_f\right)}{\eta\cos\left(\gamma_T-\gamma_f\right)-1} \tag{15}$$

From Eq. (15), FOV limit could restrict the triangle condition satisfying the lock-on condition. The following analysis provides the set of achievable impact angle set.

3.1.1 Case 1: $a<1$ (Wide FOV limit)

In this case, the achievable impact angle set when the seeker has a wide FOV is shown. The terminal look angle satisfying the collision triangle condition can be obtained from Eq. (15) by ignoring FOV limit as

$$\tan\sigma_f\in\left[\frac{-\eta}{\sqrt{1-\eta^2}},\frac{\eta}{\sqrt{1-\eta^2}}\right] \tag{16}$$

From $a=\eta/\sin\sigma_{\max}<1$, the look angle limit has the following relation

$$\tan\sigma_{\max}>\frac{\eta}{\sqrt{1-\eta^2}} \tag{17}$$

Since the terminal look angle can be selected to be within the FOV limit, FOV limit may not restrict the interception of the target. In other words, the achievable impact set can be

determined by the look-angle constraint-free guidance law. Using PPN guidance, for example, the achievable impact set for moving target can be obtained as ([7])

$$\gamma_f \in \left[\gamma_f^* \quad \lambda_0 + \sin^{-1}\left(\mp \frac{V_T}{V_M} \sin\lambda_0 \right) \right] \quad (18)$$

where subscript o denotes an initial condition, and $\gamma*$ is given by

$$\frac{\sin\gamma_f^*}{\cos\gamma_f^* \mp V_T / V_M} = \tan\left(\frac{\gamma_f^* - \gamma_0}{N} + \lambda_0 \right) \quad (19)$$

Note that if the missile maintains the constant look-angle, $\tan^{-1}\left(\frac{\eta}{\sqrt{1-\eta^2}} \right) < \sigma_0 < \sigma_{\max}$ during the maneuver, then the missile reaches a maximum acceleration before intercepting the target.

3.1.2 Case 2: $a > 1$ (Narrow FOV limit)

When the FOV limit is narrow so that the magnitude of the parameter is larger than unity, i.e., $a > 1$, the FOV limit has the following inequality.

$$\tan\sigma_{\max} < \frac{\eta}{\sqrt{1-\eta^2}} \quad (20)$$

Since the FOV limit does not cover the achievable terminal look angle set (16), the achievable terminal look angle set is reduced as

$$\tan\sigma_f \in \left[-\tan\sigma_{\max}, \tan\sigma_{\max} \right] \quad (21)$$

Therefore, the achievable impact angle set corresponding to the achievable look angle set is reduced according to the FOV limit. The following proposition addresses the reduced impact angle set.

Proposition 1. Suppose that a missile engages a non-maneuvering target with $a = \eta / \sin\sigma_{\max} > 1$, and $\sigma \in \left[-\sigma_{\max}, \sigma_{\max} \right]$. Then, achievable impact angle set is restricted by

$$\gamma_{m_f} \in \left[\gamma_{\min}^* \quad \gamma_{\max}^* \right] \quad (22)$$

where the lower bound and upper bound of the achievable impact angle set satisfy

$$\tan\sigma_{(\cdot)} = \frac{\eta \sin\left(\gamma_T - \gamma_{(\cdot)_f}^* \right)}{\eta \cos\left(\gamma_T - \gamma_{(\cdot)_f}^* \right) - 1} \quad (23)$$

where $(\cdot)$ denotes min or max.

3.2 Feasible trajectory analysis

In this section, the allowable capture region is examined by deriving a feasible trajectory. Note that the FOV limit does not restrict the achievable impact angle set when the seeker has wide FOV. Let us focus our interest on the small FOV case, i.e., $a > 1$.

Since the maximum maneuver of the missile can be restricted by the deviated pursuit trajectory, the qualitative characteristics is closely related to the pursuit maneuver. Given initial relative position (r_0, λ_0), the maximum and minimum trajectory steered by the pursuit guidance can be obtained using Eqs. (9) and (10) as

$$r_{\max} = r_0 \frac{V_T \sin\left(\gamma_T - \lambda_0 \right) + V_m \sin\sigma_{\max}}{V_T \sin\left(\gamma_T - \lambda \right) + V_m \sin\sigma_{\max}} \times \exp\left(-\frac{2\cot\sigma_{\max}}{\sqrt{a^2-1}} \tanh^{-1}\left(\frac{\tan\left(\frac{\gamma_T - \lambda}{2} \right) + a}{\sqrt{a^2-1}} \right) \Bigg|_{\lambda_0}^{\lambda} \right) \quad (24)$$

$$r_{\min} = r_0 \frac{V_T \sin\left(\gamma_T - \lambda_0 \right) + V_m \sin\sigma_{\min}}{V_T \sin\left(\gamma_T - \lambda \right) + V_m \sin\sigma_{\min}} \times \left[\exp\left(-\frac{2\cot\sigma_{\min}}{\sqrt{a^2-1}} \tanh^{-1}\left(\frac{\tan\left(\frac{\gamma_T - \lambda}{2} \right) + a}{\sqrt{a^2-1}} \right) \Bigg|_{\lambda_0}^{\lambda} \right) \right] \quad (25)$$

Thus, the feasible missile trajectory using the look-angle constraint guidance command can be bounded by the maximum and minimum trajectory obtained by Eqs. (24) and (25). Figure 5 shows the feasible trajectory for the tail chase

and head on engagements in LOS polar coordinate. In Fig. 5, shaded area denotes the feasible trajectory envelope, and dotted line represents maximum acceleration boundary. Since the boundary of the feasible trajectory envelope has the property that it diverges from the desired collision course in head-on case, the missile reaches its maximum acceleration limit before reaching the target and finally fails to interception.

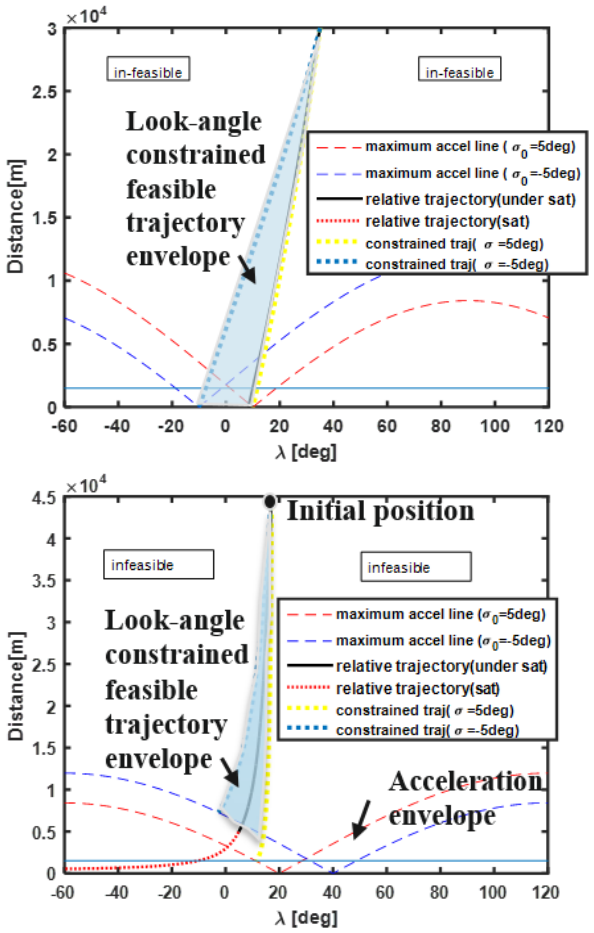

Figure 5 Feasible trajectory envelope

Based on the feasible trajectory envelope, a necessary condition for the capture region can be derived by excluding an un-capturable region for the head-on engagement. Assume that the missile maneuver is governed by a pursuit guidance to maintain its look angle limit, then the missile trajectory can reach its maximum acceleration envelope. Let us define an allowable miss-distance r_f. Then, λ_f for the r_f is calculated to obtain the intersection point between the allowable distance and the acceleration limit boundary. Combined with the acceleration limit, the allowable capture region can be obtained by backward integrating the pursuit-trajectory from allowable distance.

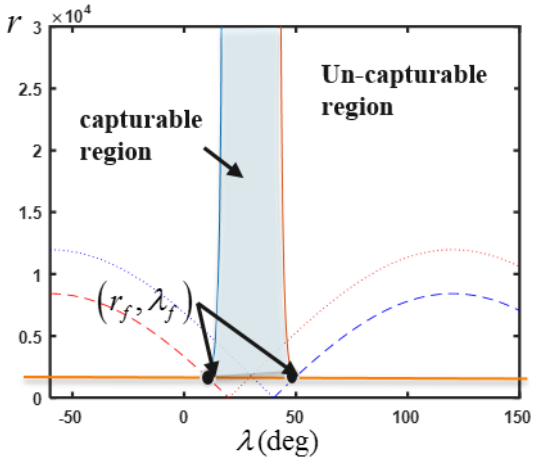

Figure 6 Allowable Capture region

Figure 6 shows the allowable capture region. In Fig. 6, the dotted line represents acceleration limit boundary, and the solid line indicates allowable miss distance. If the missile is located outside the shaded area, then the missile cannot intercept the target while maintaining lock-on condition for any look-angle constraint guidance laws. Therefore, the shaded area can be regarded as the capturable region considering the FOV constraint of the seeker.

4. Numerical Simulation

To validate the capture region analysis, numerical simulation is carried out considering the narrow FOV condition. In the simulation scenario, missile speed is faster than target speed, and the FOV is ±5 degree. Initial condition and other parameters are summarized in Table 1.

For comparison, switching guidance law [1,7] and proportional navigation guidance (PNG) law are chosen as look angle constraint guidance law and constraint-free guidance, respectively. Figures 7-9 show simulation results for the tail-chase scenario. As shown in Fig. 8, missile trajectory using the look angle constraint guidance lies in the feasible trajectory envelope. The missile intercepts the target while maintaining lock-on condition during the engagement. Compared to the PN guidance law,

the look angle of the missile is remained within the FOV during the flight, and the terminal impact angle and LOS are also properly constrained.

Figures 10-12 show the simulation result for the scenario 2. The trajectories using the constraint guidance law lie in the feasible envelope until the missile reaches its acceleration limit. Compared to the PN guidance, the maneuver using the look angle constraint guidance law is restricted to make the look angle remain within the FOV. It involves large miss-distance as shown in Figs. 10 and 12. Because the initial position of the missile is in the un-capturable region, the both guidance commands cannot intercept the target and do not satisfy the lock-on condition.

In the scenario 3, where the missile is located in the capturable region. As shown in Figs. 13-15, the missile can intercept the target while maintaining the lock-on condition.

Table 1 Simulation parameter

Target initial position	$(6{,}000,\ 20{,}000)$ (m)
Target speed	$V_T = 1000$ m/s
Missile speed	$V_m = 2000$ m/s
Look-angle limit	$\sigma_{\max} = 5\,\text{deg}$
Acceleration limit	$a_{\max} = 20g$
Scenario 1 (Tail-chase)	
Target flight-path angle	$\gamma_T = 0$
Initial relative position (Missile)	$R = 50km, \lambda_0 = 20\,\text{deg}$
Scenario 2 (Head-on 1)	
Target flight-path angle	$\gamma_T = 210\,\text{deg}$
Initial relative position (Missile)	$R = 30km, \lambda_0 = 15\,\text{deg}$
Scenario 3 (Head-on 2)	
Target flight-path angle	$\gamma_T = 210\,\text{deg}$
Initial relative position (Missile)	$R = 30km, \lambda_0 = 38\,\text{deg}$

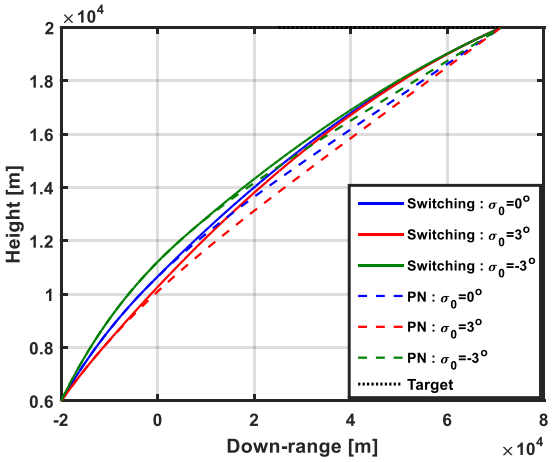

Figure 7 Missile and Target trajectory (Scenario 1)

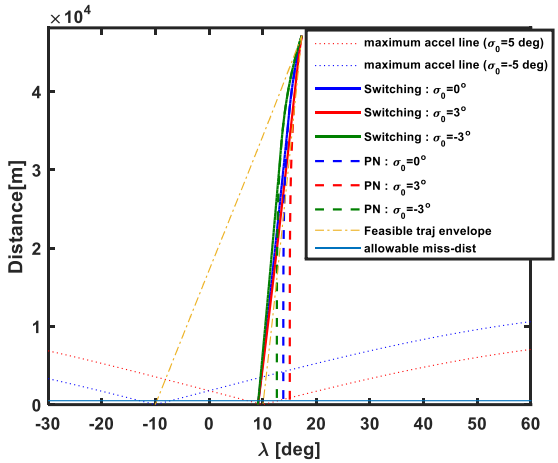

Figure 8 Relative trajectory (LOS coordinate, Scenario 1)

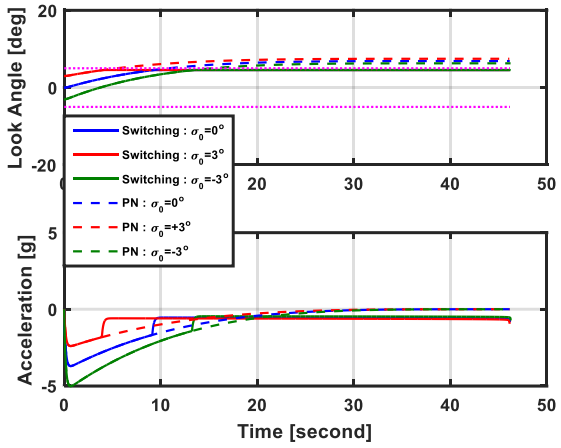

Figure 9 Time history of Look angle and acceleration (Scenario 1)

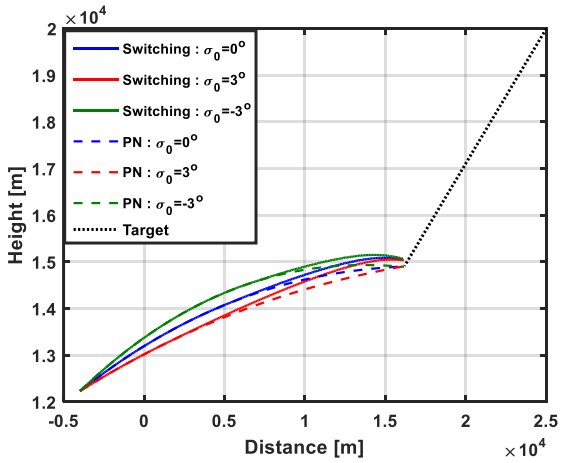

Figure 10 Missile and Target Trajectory (Scenario 2)

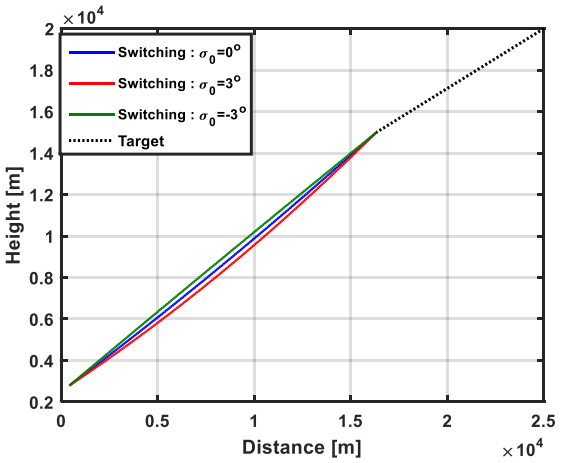

Figure 13 Missile and Target Trajectory (Scenario 3)

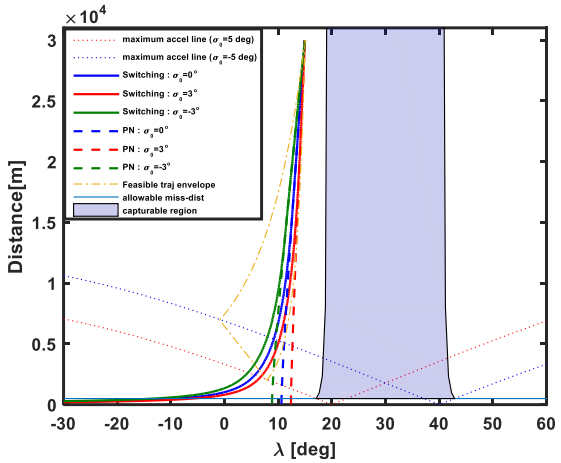

Figure 11 Relative trajectory (LOS coordinate, Scenario 2)

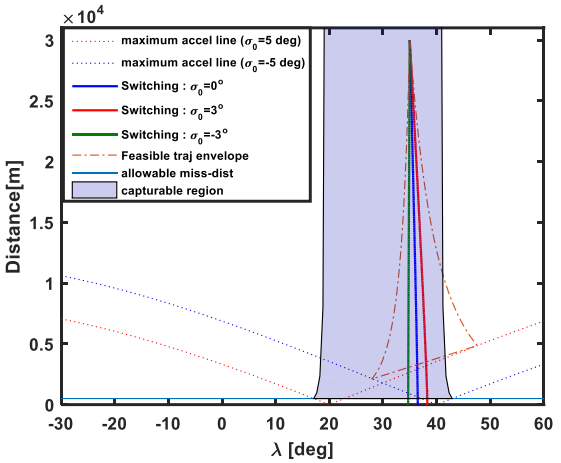

Figure 14 Relative trajectory (LOS coordinate, Scenario 3)

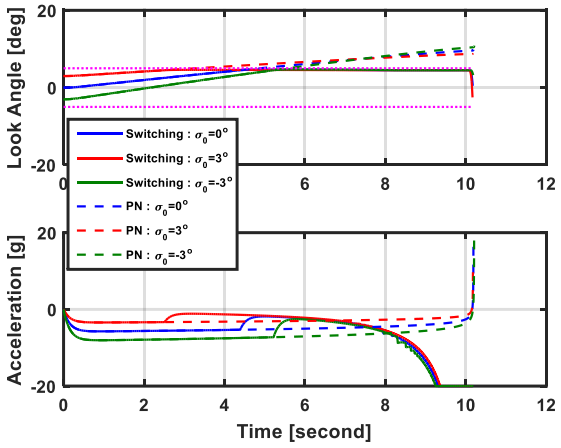

Figure 12 Time history of Look angle and acceleration (Scenario 2)

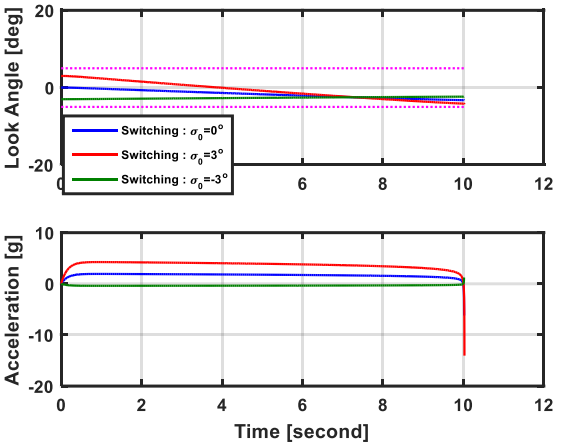

Figure 15 Time history of Look angle and acceleration (Scenario 3)

5. Conclusion

Capture region analysis was performed considering the FOV limit of the seeker. In the consideration of physical constraints including FOV limit and maximum acceleration, the feasible trajectory envelope was analytically derived, and achievable impact angle set and capturable region were analyzed. When the FOV is narrow, the shrunk feasible trajectory envelope restricts the missile maneuver and reduces capture region. Based on the analysis, impact angle control guidance law will be designed for the future work.

Acknowledgement

This work was conducted at High-Speed Vehicle Research Center of KAIST with the support of Defense Acquisition Program Administration (DAPA) and Agency for Defense Development (ADD).

References

[1] D. K. Sang and M. J. Tahk, “Guidance Law Switching Logic Considering The Seeker`s Field-of View Limits,” Proceeding of the Institution of Mechanical Engineers, Part G: Journal of Aerospace Engineering, Vol. 223, No. 8, 2009, pp. 1049-1058.

[2] A. Ratnoo, “Analysis of Two-Stage Proportional Navigation with Heading Constraints,” Journal of Guidance, Control, and Dynamics, Vol. 39, No. 1, 2016, pp. 156-164.

[3] K. Erer, R. Tekin, and M. Ozgoren, “Look-angle Constrained Impact Angle Control Based on Proportional Navigation,” AIAA Guidance, Navigation, and Control Conference, Kissimmee, FL, Jan. 2015.

[4] B. Park, T. Kim, and M. J. Tahk, “Optimal Impact Angle Control Guidance Law Considering the Seeker’s Field-of-View Limits,” Proceeding of the Institution of Mechanical Engineers, Part G: Journal of Aerospace Engineering, Vol. 227, No. 8, 2013, pp. 1347-1364.

[5] T. H. Kim, B. G. Park, and M. J. Tahk, “Bias-Shaping Method for Biasd Proportional Navigation with Terminal-Angle Constraint,” Journal of Guidance, Control, and Dynamics, Vol. 36, No. 6, 2013, pp. 1810-1815.

[6] C. H. Lee, C Hyun, J. G. Lee, and J. Y. Choi, “A Hybrid Guidance Law for a Strapdown Seeker to Maintain Lock-on Conditions against High Speed Targets,” Journal of Electronic Engineering Technology, Vol. 8, No. 1, 2013, pp. 190-196.

[7] B. Park, H. Kwon, Y. Kim, and T. Kim, “Composite Guidance Scheme for Impact Angle Control Against a Nonmaneuvering Moving Target,” Journal of Guidance, Control, and Dynamics, Vol. 39, No. 5, 2016, pp. 1129-1136.

Contact Author Email Address

- Seokwon Lee
(mailto: blueswl@snu.ac.kr)
- Youdan Kim (corresponding author, mailto: ydkim@snu.ac.kr)
- Tae-Yoon Um
(mailto: uty20000@daum.net)

Copyright Statement